Fine Structure of the Giant $M1$ Resonance in ^{90}Zr

G. Rusev,[1,2,*] N. Tsoneva,[3,4] F. Dönau,[5] S. Frauendorf,[5,6] R. Schwengner,[5] A. P. Tonchev,[1,2,†] A. S. Adekola,[2,7,‡] S. L. Hammond,[2,7] J. H. Kelley,[2,8] E. Kwan,[1,2,†] H. Lenske,[3] W. Tornow,[1,2] and A. Wagner[5]

[1]*Department of Physics, Duke University, Durham, North Carolina 27708, USA*
[2]*Triangle Universities Nuclear Laboratory, Durham, North Carolina 27708, USA*
[3]*Institut für Theoretische Physik, Universität Gießen, 35392 Gießen, Germany*
[4]*Institute for Nuclear Research and Nuclear Energy, 1784 Sofia, Bulgaria*
[5]*Institut für Strahlenphysik, Helmholtz-Zentrum Dresden-Rossendorf, 01314 Dresden, Germany*
[6]*Department of Physics, University of Notre Dame, Notre Dame, Indiana 46556, USA*
[7]*Department of Physics and Astronomy, The University of North Carolina at Chapel Hill, Chapel Hill, North Carolina 27599, USA*
[8]*Department of Physics, North Carolina State University, Raleigh, North Carolina 27695, USA*

(Received 2 March 2012; published 9 January 2013)

The $M1$ excitations in the nuclide ^{90}Zr have been studied in a photon-scattering experiment with monoenergetic and linearly polarized beams from 7 to 11 MeV. More than 40 $J^\pi = 1^+$ states have been identified from observed ground-state transitions, revealing the fine structure of the giant $M1$ resonance with a centroid energy of 9 MeV and a sum strength of 4.17(56) μ_N^2. The result for the total $M1$ strength and its fragmentation are discussed in the framework of the three-phonon quasiparticle-phonon model.

DOI: 10.1103/PhysRevLett.110.022503 PACS numbers: 23.20.Lv, 21.60.Jz, 25.20.Dc, 27.60.+j

The long-standing controversy on the nature and spectral distribution of the nuclear magnetic transition strength is a subject of continuous interest [1–4]. As a general observation, measurements find considerably less magnetic strength than theoretically expected. This is known as the quenching phenomenon of the nuclear spin-flip magnetic response. Explaining the dynamics of quenching means to understand the coupling of the two-quasiparticle doorway states to many-quasiparticle configurations. For that goal, we have to distinguish two contributions: there are wave function and vertex renormalization effects which are affected by the full reservoir of many-quasiparticle states, including those that are far away in energy. In addition, there is a fragmentation pattern seen in the measured spectral region, reflecting directly both the level density of background states and the strength of dissipative coupling. Theoretically, the description of the fine structure, however, requires us to analyze the 1^+ spectrum by accounting for core polarization effects. Because any one of such calculations will be based on limited model spaces, the theoretical results can only predict a lower limit of quenching. Hence, we have to expect to overpredict the measured strength to some extent. That overestimate is taken care of by an additional phenomenological quenching factor q, where $1\text{-}q$ indicates the amount of strength located outside the model space accounting also for the contributions from the hard scale of mesonic and subnucleonic degrees of freedom. In this sense, a reliable description of the fragmentation pattern of the magnetic dipole ($M1$) response function is important for understanding the spin dynamics of the nucleus.

In this Letter, we intend to contribute to the solution of these problems by reporting on the first high-resolution study of the $M1$-giant resonance (GR) fragmentation. For that purpose, a nucleus like ^{90}Zr is well suited because the core polarization mechanism responsible for the quenching phenomenon is stronger in nuclei where the jj-coupling scheme prevails.

We observed numerous $J^\pi = 1^+$ states in ^{90}Zr populated in a photon-scattering experiment at the High-Intensity γ-ray Source (HIγS) facility. Additionally, the experiment aimed at providing the most accurate value for the total $M1$ strength in ^{90}Zr in the region of the $M1$-GR. Analysis of the data involved many-body calculations using mean-field and random-phase approximation (RPA) techniques of the extended quasiparticle-phonon model (QPM) approach as discussed in Refs. [5,6]. An interesting result of our work, which sheds light on the magnetic transition operator, is that multiparticle multihole effects increase strongly the orbital part of the magnetic transition operator.

The $M1$-GR in ^{90}Zr has been studied extensively in proton- and electron-scattering experiments [7,8]. Observation of a broad structure around 9 MeV revealed the total $M1$ strength of the resonance, but the poor resolution of the charge-particle spectrometers prevented identification of the individual 1^+ levels. However, the few levels observed in high-resolution scattering experiments of electrons [9] and polarized protons [10] confirmed that the $M1$ strength in ^{90}Zr is highly fragmented. The large background and high fragmentation of the $M1$ strength cause doubt in the accuracy of the published total $M1$-GR strength [11]. Another problem in charged-particle scattering experiments is the correct assignment of spin and parity values for the observed levels. Most of the strength found in (p, p') experiments was assigned $M2$ character based on high-resolution (e, e') measurements, instead of $M1$ (see Ref. [12]).

The study of the $M1$-GR structure requires a reaction which selectively populates dipole states and allows for unique spin and parity assignments of the levels. The HIγS facility of the Triangle Universities Nuclear Laboratory produces 100% linearly polarized and nearly monoenergetic photon beams using intercavity Compton backscattering of free-electron laser beams with electrons stored in a storage ring. Experiments at the HIγS facility provide the opportunity to (i) excite low-spin levels (mainly dipole), (ii) assign the spin and parity of those levels by measuring the scattered γ rays at two different polar angles and two different azimuthal angles (see, e.g., Refs. [13,14]), and (iii) distinguish between ground-state and branching transitions, i.e., to determine the level scheme. Due to the monochromaticity of the beam, the background resulting from atomic scattering processes of the incident photons within the target appears below the energy range of levels excited by the beam, which enhances the detection sensitivity for measuring the elastic-scattering ground-state transitions [15].

The dipole excitations in ^{90}Zr were studied at energies from 7 to 11 MeV. The energy distribution of the photon beam was measured with a 123% efficient high-purity Ge detector placed in the beam. This distribution is compared in Fig. 1(a) with the flux deduced from the strong $E1$ transitions in ^{90}Zr of known strength [16]. The γ rays scattered from a 4054.2-mg $^{90}ZrO_2$ sample were measured with four 60% high-purity Ge detectors. Two of the detectors were positioned in the plane perpendicular to the beam, one of them vertically (90°, 90°) and the other horizontally (90°, 0°). This configuration allows for distinction between $M1$ and $E1$ transitions. The other two detectors were positioned in the horizontal plane at the backward angle of $\theta = 135°$ relative to the beam, in order to discriminate $M1$ transitions of particular interest from $E2$ transitions. At all energies, measurements were performed with a total photon flux of 5×10^7 s^{-1} for about 5 h. Spectra of γ rays scattered from the ^{90}Zr sample in the three directions are shown in Fig. 1 for the beam energy of 9.2 MeV.

The present experiment provides for the first time precise information about the distribution of 1^+ states and its $M1$ strength in the hitherto inaccessible energy region above an excitation energy of 6 MeV. Reduced transition probabilities, $B(M1)$, of the newly observed $M1$ de-excitations were deduced by normalizing the products of photon flux and detection efficiency to values obtained from the integrated scattering cross sections of the $E1$ transitions in ^{90}Zr [16]. This normalization method omits the need for using the absolute flux and absolute efficiency. All observed peaks with energies within the energy distribution of the beam correspond to ground-state transitions; i.e., they result from and define excited levels because of the high energy of the first excited state in ^{90}Zr ($E_{0^+} = 1.761$ MeV). The deduced $B(M1)$ values obtained in the present work are shown in Fig. 2(a). They

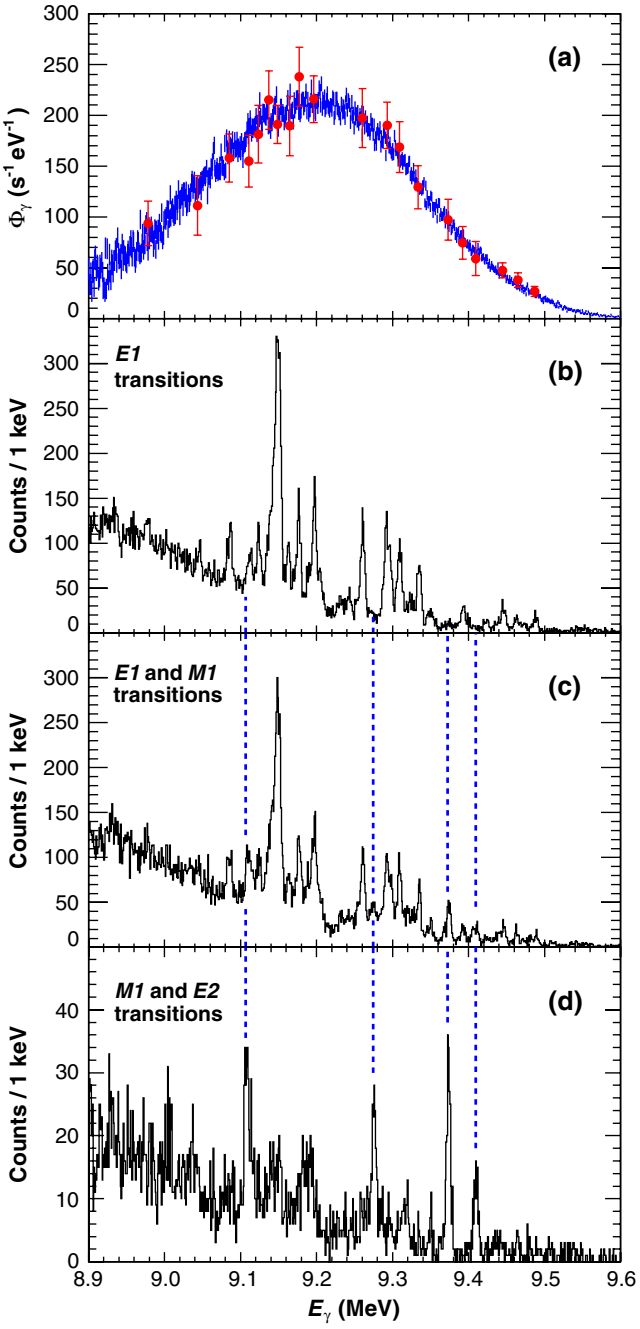

FIG. 1 (color online). (a) Energy distribution of the incident photon beam (the vertical error bars represent statistical uncertainties) normalized to the flux deduced from strong $E1$ transitions of ^{90}Zr, shown as data points. Measured spectra at (θ, ϕ) of (90°, 90°) (b) containing $E1$ transitions, of (135°, 0°) (c) and of (90°, 0°) (d) containing mostly $M1$ transitions. The vertical blue lines show some of the strong $M1$ transitions.

characterize the isovector $M1$ resonance in ^{90}Zr with a centroid energy of 9.0 MeV and a sum strength of 3.17(8) μ_N^2. Cascade simulations for ^{90}Zr described in Ref. [16] give a 76(10)% mean branching ratio for ground-state transitions of 1^+ levels in the considered energy range. Correcting the measured strength for this branching

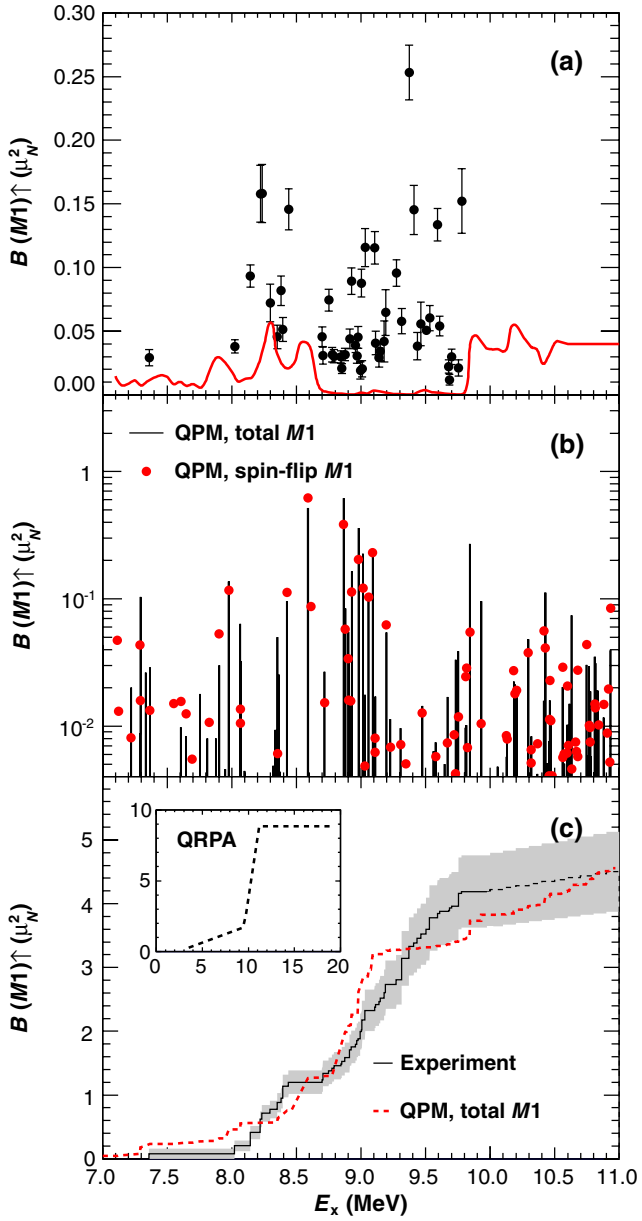

FIG. 2 (color online). Results for (a) the measured $B(M1)$ strength of discrete levels in ^{90}Zr compared with the detection limits (red solid line) and (b) predictions from the quasiparticle-phonon model. A comparison of the measured and calculated QPM cumulative $M1$ strength is shown in panel (c). The dashed line continuing the solid line above 10 MeV represents the $M1$ strength obtained from the continuum. The shaded area gives the uncertainty of the experimental values. QRPA results of the total cumulative $M1$ strength up to 20 MeV are shown in the insert.

ratio, we obtain $\Sigma B(M1) = 4.17(56)\mu_N^2$. Because discrete peaks above 10 MeV have not been observed, we estimated the $M1$ strength from the continuum to be $\Sigma_{10\,\mathrm{MeV}}^{11\,\mathrm{MeV}} B(M1)_{\mathrm{Exp.}} \uparrow = 0.31(16)\mu_N^2$.

Theoretical approaches based on the widely used RPA, second RPA [17], extended RPA [18], and the multiconfiguration shell model commonly suggest that at energies above 6 MeV, the $M1$ strength is dominated by strong single-particle spin-flip transitions. Realistic shell-model calculations analogous to the ones described in Ref. [19] with an effective spin g factor $g_{\mathrm{eff}}^s = 0.8 g_{\mathrm{bare}}^s$ predict three 1^+ states around 7 MeV dominated by the $\nu(g_{9/2}^{-1} g_{7/2})$ spin-flip excitation with a total strength of 6.9 μ_N^2, where the contribution of this component to the wave functions is of about 25%. In comparison, we calculated a strength of $15\mu_N^2$ for the pure neutron $\nu(g_{9/2}^{-1} g_{7/2})$ spin-flip excitation using the independent-particle model with g_{bare}^s. Obviously, these models describe those excitations only within certain limits. The fragmentation problem requires more detailed investigations than possible with two-quasiparticle or one-phonon approaches.

An understanding of the experimentally observed fine structure of the magnetic response is expected to require the detailed treatment of the multiquasiparticle and multiphonon structure of the 1^+ excited states. For this purpose, calculations in the framework of an extended version of the QPM [6] have been performed to investigate the fragmentation pattern of the $M1$ strength below and around the neutron-emission threshold in ^{90}Zr. The present calculations are in line with our previous QPM results on $E1$ transitions in this nucleus [16], as well as with $E1$ and $E2$ studies in other nuclei [6,14,20]. However, the approach is improved by expanding the multiphonon model space to include unnatural parity states, so-called magnetic excitations with parity $\pi = (-)^{J+1}$, instead of the usual restriction to natural parity states only with $\pi = (-)^J$. As a result, the model basis is constructed of one-, two-, and three-phonon states with J^π from $1^\pm$ to $7^\pm$ and excitation energies of up to 11 MeV. For numerical reasons, the QPM configuration space is reduced by the exclusion of very small coupling matrix elements, usually related to noncollective phonons [21].

The aforementioned still-open problems regarding the theory of nuclear magnetic transitions are also of relevance to our analysis. However, among the effects contributing to the deviation of static and transition moments from the naively expected values, we are confident in our understanding of the genuine many-body effects originating from core polarization [22]. We expect this part to be accounted for by our QPM calculations with up to three (microscopically described) phonon configurations, covering explicitly the major part of nuclear many-body effects acting on the low-energy scale. However, modifications of the transition operators due to the coupling to configurations outside of the model space and those induced by mesonic and subnucleonic degrees of freedom remain unaccounted for. Since those effects are connected with energy and momentum scales much different from the nuclear low-energy region, they are taken into account globally by a renormalization of the spin g factor. Following previous QPM calculations [23], the $M1$ transitions are calculated with a quenched effective

spin-magnetic factor $g^s_{\rm eff} = 0.8 g^s_{\rm bare}$, where the bare spin-magnetic moment is denoted by $g^s_{\rm bare}$. The QPM calculations were performed as in Ref. [16] with single-particle energies obtained from Hartree-Fock-Bogoliubov calculations and a residual two-quasiparticle interaction of separable form with empirical parameters [21]. An exception to this prescription is that the isovector spin-dipole coupling constant is obtained from fully self-consistent quasiparticle-RPA (QRPA) calculations using the microscopic energy-density functional of Ref. [24]. The distribution of the calculated $M1$ strength is shown in Fig. 2(b).

The analysis of the QRPA $M1$ strength of 1^+-state excitations with energies up to 20 MeV indicates that it is mostly due to single p-h spin-flip states. The relatively large QRPA contribution of the orbital $M1$ strength, which is related to the lowest-lying $1^+_{\rm QRPA}$ state at 3.51 MeV, is about 20% of the total $B(M1)\uparrow = 0.28\mu_N^2$ of that state. Nevertheless, the total orbital QRPA strength for the whole energy range up to 20 MeV is very small, less than 2% of the total QRPA $M1$ strength. An additional interference between spin and orbital strengths leads to the suppression of the total $M1$ response. An exception is the $1^+_{\rm QRPA}$ state at 9.75 MeV, where a constructive interference and an enhancement of the total $M1$ strength is observed.

The phonon-coupling leads to two distinct effects: (i) fragmentation by coupling to multiphonon states within the considered energy interval and (ii) dynamical redistribution of the transition strength by shifting part of the strength to higher energies. The detailed studies of the $M1$ fragmentation pattern based on QPM multiphonon calculations indicate that the coupling of natural parity phonons to multiphonon 1^+ states induces an additional orbital contribution to the $M1$ transitions. The calculated $M1$ strength at excitation energies between 7 and 11 MeV contains a considerable orbital part (obtained by setting $g^s_{\rm eff} = 0$) of about 22% of the total $M1$ strength. In fact, the two-phonon orbital strength is about 10 times larger than QRPA orbital strength. For comparison, the ratio for spin-flip transitions is on the order of 0.1. The sizable enhancement of the orbital part of the $M1$-matrix elements is on first sight unexpected. A detailed analysis of the QPM results shows that the increase is caused by the core polarization effects described by the multiphonon coupling. The phonon coupling shifts down part of the transition strength of a known strong $M1$ state, located in our calculations at $E = 11.2$ MeV. This accounts for about half of the increase of the total $M1$ strength; however, it contributes about a few percent of its orbital part. The main increase of the orbital $M1$ strength is related to transitions from multiphonon ground-state correlations. It is well established that the orbital $M1$ strength increases with deformation [25]. The multiphonon ground-state correlations can be considered as shape fluctuations, expected to increase the orbital $M1$ strength in a similar way. A corresponding effect was found in connection with the 2^- twist mode [26]. In the energy region considered here the two-phonon parts of the mixed $M1$ eigenstates are dominated by a single or a few two-phonon states. Hence, suppression of the two-phonon components by random phase averaging as observed in other cases, e.g., Ref. [27] does not take place. The analysis of the fine structure of the distribution of one- and two-phonon spin-flip and orbital $M1$ strengths in ^{90}Zr indicates that the observed $M1$ strength below 11 MeV can be separated in different parts by means of the structure of the contributing transitions [cf. Fig. 2(b)]. Thus, at energies below 8 MeV the 1^+ excited states are strongly mixed with almost equal contributions of one-phonon spin-flip and two-phonon orbital transitions. An exception is the energy region from 7.2 to 7.8 MeV, where a small concentration of the spin-flip strength is related to the fragmented tail of the decay pattern of the 1^+_2 and 1^+_3 QRPA states, respectively. At energies between 8 and 11 MeV the one-phonon spin-flip transitions clearly dominate over the two-phonon contributions for both the spin-flip and orbital components. Nevertheless, the latter contributions should not be neglected. This is a highly interesting finding, theoretically and experimentally.

The total QPM $M1$ strength summed over the 1^+ states is $\Sigma^{11\,\rm MeV}_{7\,\rm MeV} B(M1)_{\rm QPM}\uparrow = 4.6\mu_N^2$ with a centroid energy $E^{\rm QPM}_{\rm c.m.} = 9.1$ MeV. The calculated strength below 7 MeV is $1\mu_N^2$. The theoretical results are in good agreement with the experimental values of $\Sigma^{7\,\rm MeV}_{11\,\rm MeV} B(M1)_{\rm Exp.}\uparrow = 4.5(6)\mu_N^2$ and $E^{\rm Exp.}_{\rm c.m.} = 9.0$ MeV, respectively. A comparison of the measured and calculated cumulative $M1$ strengths is shown in Fig. 2(c).

Of special interest is the behavior of the $M1$ strength at higher energies, namely in the range of 11 to 12.5 MeV. At these energies, which include the neutron-separation energy ($S_n = 11.97$ MeV), the experimental accessibility is strongly reduced. However, we can explore this region theoretically in the QPM by including one- and two-phonon configuration spaces with energies up to 12.5 MeV. The model predicts a strongly fragmented $M1$ strength, related mainly to the decay of the 1^+_4 (QRPA) state into a considerable number of relatively uniformly distributed 1^+ states with very small transition probabilities, typically less than $0.2\mu_N^2$, and a total strength $\Sigma^{12.5\,\rm MeV}_{11\,\rm MeV} B(M1)\uparrow \approx 2\mu_N^2$. The existence of 1^+ states near the neutron-separation energy has been reported in Ref. [28].

In summary, an experiment determining the structure of the $M1$-GR below the neutron-separation energy has been carried out on ^{90}Zr at the HIγS facility. A resonancelike concentration of 1^+ states centered at 9 MeV was identified. The concentration of $M1$ strength around 9 MeV is further confirmed in three-phonon QPM calculations and explained as fragmented spin-flip excitations. The observed strongly fragmented $M1$ strength and its absolute value can be explained only if more complex excitations than the single particle-hole ones are taken into account.

The theoretical investigations of the fragmentation pattern of the $M1$ strength indicate a strong increase of the contribution of the orbital part of the magnetic moment due to coupling of multiphononon states. The effect is estimated to account for about 22% of the total $M1$ strength below the threshold. The good agreement of the calculated and measured total strengths is a signature that the quenching is handled reliably in the chosen approximation. A better understanding could be achieved with more comprehensive knowledge of the nature of the intrinsic nuclear moments and meson-exchange currents, which might be of importance for additional improvements.

This work was supported in part by the US Department of Energy under the Grants No. DE-FG02-97ER41033, No. DE-FG02-97ER41041, No. DE-FG02-97ER41042, and No. DE-FG02-95ER40934, and the BMBF Project No. 06GI9109.

*Present address: Chemistry Division, Los Alamos National Laboratory, Los Alamos, New Mexico 87545, USA.

†Present address: Physics Division, Lawrence Livermore National Laboratory, Livermore, California 94551, USA.

‡Present address: Canberra Industries, Inc., Meriden, Connecticut 06450, USA.

[1] A. Arima and H. Horie, Prog. Theor. Phys. **11**, 509 (1954).
[2] A. Bohr and B. Mottelson, *Nuclear Structure* (Benjamin, New York, 1975).
[3] W. Weise, Prog. Part. Nucl. Phys. **11**, 123 (1984).
[4] I. S. Towner, Phys. Rep. **155**, 263 (1987).
[5] N. Tsoneva, H. Lenske, and Ch. Stoyanov, Phys. Lett. B **586**, 213 (2004).
[6] N. Tsoneva and H. Lenske, Phys. Rev. C **77**, 024321 (2008).
[7] F. Osterfeld, Rev. Mod. Phys. **64**, 491 (1992).
[8] K. Heyde, P. von Neumann-Cosel, and A. Richter, Rev. Mod. Phys. **82**, 2365 (2010).
[9] D. Meuer, R. Frey, D. H. H. Hoffmann, A. Richter, E. Spamer, O. Titze, and W. Knüpfer, Nucl. Phys. **A349**, 309 (1980).
[10] S. K. Nanda *et al.*, Phys. Rev. Lett. **51**, 1526 (1983).
[11] R. M. Laszewski and R. Alarcon, Phys. Rev. Lett. **60**, 1202 (1988).
[12] R. M. Laszewski, R. Alarcon, and S. D. Hoblit, Phys. Rev. Lett. **59**, 431 (1987).
[13] R. Longland, C. Iliadis, G. Rusev, A. P. Tonchev, R. J. deBoer, J. Görres, and M. Wiescher, Phys. Rev. C **80**, 055803 (2009).
[14] A. P. Tonchev, S. L. Hammond, J. H. Kelley, E. Kwan, H. Lenske, G. Rusev, W. Tornow, and N. Tsoneva, Phys. Rev. Lett. **104**, 072501 (2010).
[15] E. Kwan *et al.*, Phys. Rev. C **83**, 041601(R) (2011).
[16] R. Schwengner *et al.*, Phys. Rev. C **78**, 064314 (2008).
[17] D. Cha, B. Schwesinger, J. Wambach, and J. Speth, Nucl. Phys. **A430**, 321 (1984).
[18] S. P. Kamerdzhiev and V. N. Tkachev, Phys. Lett. **142B**, 225 (1984).
[19] R. Schwengner *et al.*, Phys. Rev. C **74**, 034309 (2006).
[20] N. Tsoneva and H. Lenske, Phys. Lett. B **695**, 174 (2011).
[21] V. Soloviev, *Theory of Complex Nuclei* (Pergamon, New York, 1976).
[22] A. Arima, Hyperfine Interact. **78**, 67 (1993).
[23] A. I. Vdovin *et al.*, Yad. Fiz. **30**, 923 (1979) [Sov. J. Nucl. Phys. **30**, 479 (1979)].
[24] F. Hofmann and H. Lenske, Phys. Rev. C **57**, 2281 (1998).
[25] W. Ziegler, C. Rangacharyulu, A. Richter, and C. Spieler, Phys. Rev. Lett. **65**, 2515 (1990).
[26] B. Reitz *et al.*, Phys. Lett. B **532**, 179 (2002).
[27] V. Y. Ponomarev, A. Vdovin, and C. Velchev, J. Phys. G **13**, 1523 (1987).
[28] C. Iwamoto *et al.*, Phys. Rev. Lett. **108**, 262501 (2012).